

IMPACT OF FE MODELING IN THE SEISMIC PERFORMANCE PREDICTION OF EXISTING RC BUILDINGS

Christos A. Zeris¹, Dimitrios Vamvatsikos², Panagiotis Giannitsas³ and
Kostas Alexandropoulos⁴

¹ National Technical University of Athens,
Zografou Campus, GR 15773, Greece
e-mail: zeris@central.ntua.gr

² University of Cyprus, P.O. Box 20537,
1678 Nicosia, Cyprus
e-mail: divamva@ucy.ac.cy

³ National Technical University of Athens,
Zografou Campus, GR 15773, Greece
e-mail: takis13gcv@hotmail.com

⁴ National Technical University of Athens,
Zografou Campus, GR 15773, Greece
e-mail: basalex@acci.gr

Key words: Reinforced concrete, Finite element modeling, Performance Based Design, Inelastic seismic design, Local inelastic response, Existing frames.

Abstract. *The choice of available finite element modeling conventions of reinforced concrete (RC) buildings may influence significantly the predicted inelastic seismic performance during the evaluation of existing RC frame redesigns. The problem is investigated by analyzing alternative models of a typical existing five-story RC frame which has been designed for moderate seismicity, using past seismic provisions. Different inelastic finite element models of the structure are established, taking into account a range of practical and more detailed finite element idealizations that range from the widely adopted concentrated plasticity elements to the more complex distributed damage fiber elements, accounting or not for large deformations, joint flexibility, bond or shear deterioration. Following static inelastic analysis, key performance global and local response indices (such as interstory drift and plastic rotations) which are adopted in Performance Based Design, are estimated, to quantify the uncertainty introduced strictly by the modeling conventions alone. It is concluded that key response indicators (collapse mechanism, capacity curve and maximum plastic rotations) can be grossly underestimated strictly due to the model alone, something that should be considered in the normative process by tight modeling guidelines and adequate safety factors.*

1 INTRODUCTION AND STATEMENT OF THE PROBLEM

Performance Based Design (PBD) methods [1,2,3] are increasingly being used for the seismic evaluation and retrofit / rehabilitation redesign of existing reinforced concrete (RC) buildings. Following inelastic static analysis procedures, these methods evaluate the adequacy of an established redesign of the structure by performing inelastic static analysis of this system for the evaluation of its modal capacity curve. Upon subsequent determination of the target performance points, acceptance of the design at the local level follows, including the reliable determination of key local demands at critical regions and components of the structure and comparison of these with experimental or empirical limits of performance.

Several sources of uncertainty are introduced during the application of this evaluation process, including: i) effects due to the excitation variability, which cannot be adequately pictured by a response spectrum envelope (frequency content, duration, rate of energy release and amplitude), ii) the elastic to inelastic response prediction relationship due to cyclic inelastic response, iii) structural aspects not directly included in the model formulation, such as material variability, memory of past loadings and environmental actions within the state of the structure at the local level and so on. In all these approaches, the determination of the inelastic performance through simplified static pushover (SPO) analyses has remained the principle method of response estimation. Lately, direct dynamic analysis evaluation procedures are being increasingly adopted to quantify the excitation variability phenomena in a rational manner [4]. Out of these uncertainties, the reliable evaluation of local inelastic response relationships with the global deformations, that still remain the key controlling parameter, is more critical for existing RC buildings, due to the way these structures were designed and detailed.

Typically, pre 90s existing RC buildings in Greece, which are of concern in this study, have been designed according to the past generations of codes, namely the 1959 norm [5], which adopted allowable stress procedures, simplified structural analysis models and no capacity design. Early structures in this group do not have shear walls, while their member dimensions are narrow. Structural materials of inferior mechanical resistance and bond characteristics compared to those currently employed were used, while, in terms of seismic detailing, no critical region reinforcement was implemented, characterizing these frames as non-conforming to current standards. As a consequence, these structures often respond in the form of a soft story mechanism and their response characteristics are limited by the local ductility capacities at the critical regions as well as the anchorage characteristics of the reinforcement. Finally, since these structures are typically (in Greece at least) infilled with clay brick masonry infills of different qualities and grades, the infill configuration plays an important role in the overall inelastic structural response.

Inelastic finite element (FE) modeling of these structures plays a key role in their seismic qualification. The problem investigated herein is to examine the impact of the FE model formulation in seismic performance prediction, as used in PBD of existing RC buildings. For this purpose, the collapse mechanism, the shape of the capacity curve and the distribution and magnitude of local plastic rotations are compared, established using different FE models adopted in practical seismic design. The influence of the FE modeling in dynamic analysis (following Incremental Dynamic Analyses) has been considered in more detail in [6].

2 DESCRIPTION OF THE RC BUILDING

2.1 Description of the structure and design details

For the purpose of this study, a typical existing five story reinforced concrete (RC) building in Greece is selected. The building is assumed to be located in the seismicity zone II of the

three zone system specified by the 1959 Greek Code [5], and is therefore designed for a service seismic base shear of 6 % its seismic weight, uniformly distributed with height; since the design code was totally based on allowable stress design checks, unfactored dead and live load coefficients are adopted in the evaluation of the seismic weight while the bending, axial and shear stresses are established from elastic cracked section analysis and verified against the allowable stress values, increased by 20% for the seismic load combinations. Following standard practice, the structure is only analyzed using equivalent static methods of analysis and simplified structural models, except the perimeter frames for which frame analysis was required.

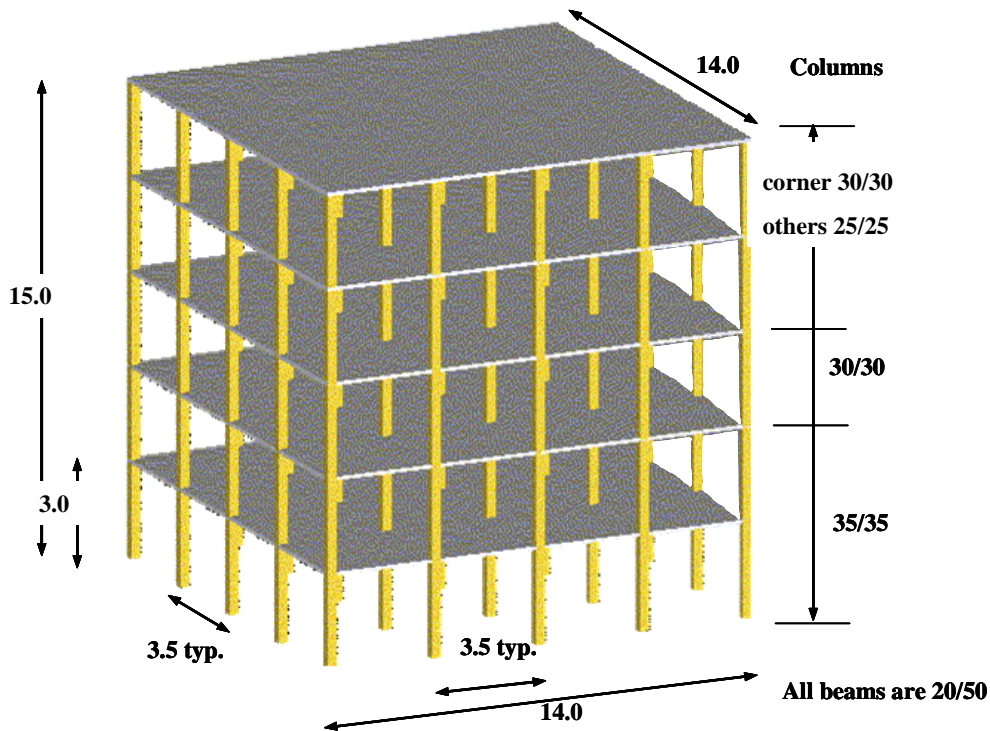


Figure 1: Schematic representation of the typical example RC building (frame dimensions in m, member dimensions in cm).

The frame is a typical representative geometry of a 60s apartment building in Greece, with narrow span dimensions and constant floor elevations, as shown in Fig. 1. The structural framing is regular in plan and elevation comprising three (transverse) by four (longitudinal) bays in plan, five stories high. The typical storey height is 3.00m wide throughout while bay sizes are 3.50m in each direction. Columns are square in section, ranging between 35x35cm at the first and second floors and 30x30cm from the third floor up, interior columns also reducing from this point up to 25x25cm. All the beams are kept to uniform section dimension of 20/50cm. Concrete slabs have a 12cm uniform thickness in all the floors and are reinforced to act in two way action. For seismic design purposes it is assumed to be founded on rock. The concrete grade used in design is B160, while the steel reinforcement consists of smooth bars of grade St I.

In addition to self weight, the design dead loads include perimeter double leaf clay masonry infill walls 25cm thick and a uniform surcharge of 2.50 kN/m², including an interior moveable partition added weight equal to 1.00 kN/m². According to the prevailing Greek Loadings Code, live load is 2.00 kN/m² for residential use. Following standard practice still in

effect in Greece, masonry infills are only introduced as inertia and vertical load only, without contributing to the lateral stiffness. Furthermore, since transverse shear reinforcement (often in the form of diagonally bent up longitudinal bars) is only used to resist service level forces, no capacity design procedures were employed either in beam or column shear force design or in the form of a joint capacity check for the establishment of a weak beam – strong column collapse pattern. Finally, no critical region confinement is used in the end critical regions, while, smooth reinforcement is employed throughout, having inferior bond characteristics.

2.2 Modeling of the structure

The building is modeled as a series of plane frames fixed at their base, taking into account the symmetry properties of the structure in the in-depth direction. In order to concentrate the present discussion to the modeling of RC behavior only, the exterior infill clay masonry panels typically used in this type of construction are currently ignored. The effect of infills to this and similar type of existing RC frames has been considered by Repapis et al. [7], through modeling of these structural forms as axially loaded diagonal compression resisting elements.

As subsequently described herein, a variety of element geometric and stiffness representations are used for the concrete member modeling, as these implemented in three nonlinear software analysis codes used, namely Drain-2DX [8], OpenSEES [9] and Seismostruct [10]. Certain modeling representations are selected at the outset for the global FE structural formulation, since both lumped plasticity member idealizations are used together with a wide variety of proposed distributed stiffness – flexibility FE models, which exhibit (at least in the way they have been implemented in the codes above) the following limitations:

i) Diaphragmatic action is everywhere imposed at each floor level through master slaving to the centre of mass. The use of continuous diaphragmatic action in every column/beam joint intersection is not possible with distributed fiber section models, due to their ability to deform axially along the reference axis, in order to account for cracking of the sections. As a consequence, the introduction of axial direction floor restraints in every node may induce significant initial stressing type axial loads, thereby modifying ultimate bending moment capacities. For this reason, only the starting lateral degrees of freedom (DOF) are interconnected at each floor between neighboring frames through model constraints, to allow for diaphragmatic action, while remaining elements rely only on their axial rigidity to transfer forces.

ii) The extent of cracking of the beams during the gravity solution phase also affects somewhat the initial redistribution of bending moments between the beams and the columns, primarily at the end bays; this effect has been investigated in more detail by imposing an initial minute axial load at each floor (of the order of 0.1% the axial load capacity of the beam sections), in order to establish initial stiffness, without affecting their inelastic resistance. Lumped models with uncoupled flexural-axial response do not require such load.

iii) Due to the inability of distributed damage FE elements, as implemented in the analysis codes considered to handle internal distributed loads, each RC beam element is discretized into five elements each, in all FE models implemented. The transverse loads from the corresponding slab tributary areas are applied as nodal loads at the interior joints so as to obtain exactly at the interior nodes the multi linear approximation of the quadratic bending moment diagram within each beam. An added advantage of this type of modeling is that mixed type collapse mechanisms (beam hinging within the span) are possible to obtain, something that would otherwise remain undetected. Since plane frame analyses are considered, out of plane beam reactions are imposed at the beam-column joints. Specifically for the multi DOF joint models – see below, nodal loads are applied at the top joint DOFs (Fig. 2).

Unlike in design, tributary vertical inertial loads equal to the dead loads plus 30% of the live load only are included in the SPO analysis, following current design conventions. Second

order effects are included following the modeling conventions of each analysis program, typically corresponding to the gravity load distribution of axial loads or updated with imposed gradual lateral deformations.

It is stressed that since the as built condition of the structure is of interest herein, average mechanical properties of the structural materials are adopted in the formulation of the structural model, as follows: the mean cylinder compressive strength of the concrete is 18 MPa while the tensile yield strength of the steel is 310 MPa, based on average test results on similar diameter StI bars, performed at the RC Laboratory of the Technical University of Athens.

2.3 Member FE modeling conventions

The FE models adopted in each case and the respective modeling discretizations (Fig.2) are as follows, depending on each of the three FE code analysis capabilities. In all cases, comparable inelastic material characteristics at the section level were specified, as these are dictated by the assumptions and limitations of the different analysis codes and the respective FE libraries these furnish. The selection of the inelastic analysis programs was arbitrary, with sole criteria of selection being the applicability of each code to perform routine SPO analyses of framed buildings for PBD, the FE library provided and the availability for desktop usage.

- Lump_1, Lump_2, (code Drain2-DX [8]): Lumped plasticity elements are used in the entire model, having end hinges with bilinear bending characteristics and axial load – bending moment interaction for the columns. Hardening is set to 5% initial stiffness (Lump_1) or 0.5% of initial for the more flexible (Lump_2) model, while the concrete modulus is equal to 28 GPa (Lump_1) or 75% of this value for the flexible model Lump_2, to allow for initial cracking. Specified inelastic hinge characteristics are obtained using equivalent bilinearizations of end critical section moment-curvature analysis, established from section analysis of fiber models, using a trilinear steel and a nonlinear softening concrete constitutive [11] law accounting for confinement. Columns are modeled using a single FE each, while five elements are used for the beam members.
- Disp_1, Disp_10, (Opensees [9]): Distributed damage elements with section monitoring along the length, at five Gauss points; the formulation adopts displacement compatibility / internal stiffness approximations, while section modeling is based on a uniaxially bent fiber representation (Fig.2). All the beams are modeled using five elements, at 0.7m apart, in order to describe accurately the reinforcement layout along the member as well as the internal force distribution under gravity. Columns are modeled using either one element per member (Disp_1) or ten elements, equally distributed per member (Disp_10). Intermediate column discretizations have been considered, as discussed later on.
- Force (Opensees [9]): Distributed damage elements with section information monitored along the length at five Gauss points; the formulation adopts force equilibrium / internal flexibility approximations, while section modeling is based on a uniaxially bent fiber representation. As in Disp_x, all the beams are modeled using five elements, at 0.7m apart. Columns are modeled using one element per member (Fig.2). Concrete and steel fiber constitutive relations in the monitored sections are identical to Disp_x.
- Disp_Large_Deformation (Seismostruct [10]): Distributed damage elements [12] with fiber section representation monitored along the length at three Gauss points (four elements per column member are used). Beams are modeled as before at 0.7m apart. Concrete and steel fiber constitutive relations are as in Disp_x.

- Constant_hinge (Opensees [9]): The structure is discretized using beam-column elements with inelastic constant hinge regions at the ends only and an elastic interior component in series. Similar section modeling is enforced as previously, while the plastic hinge length is equal to the member depth.

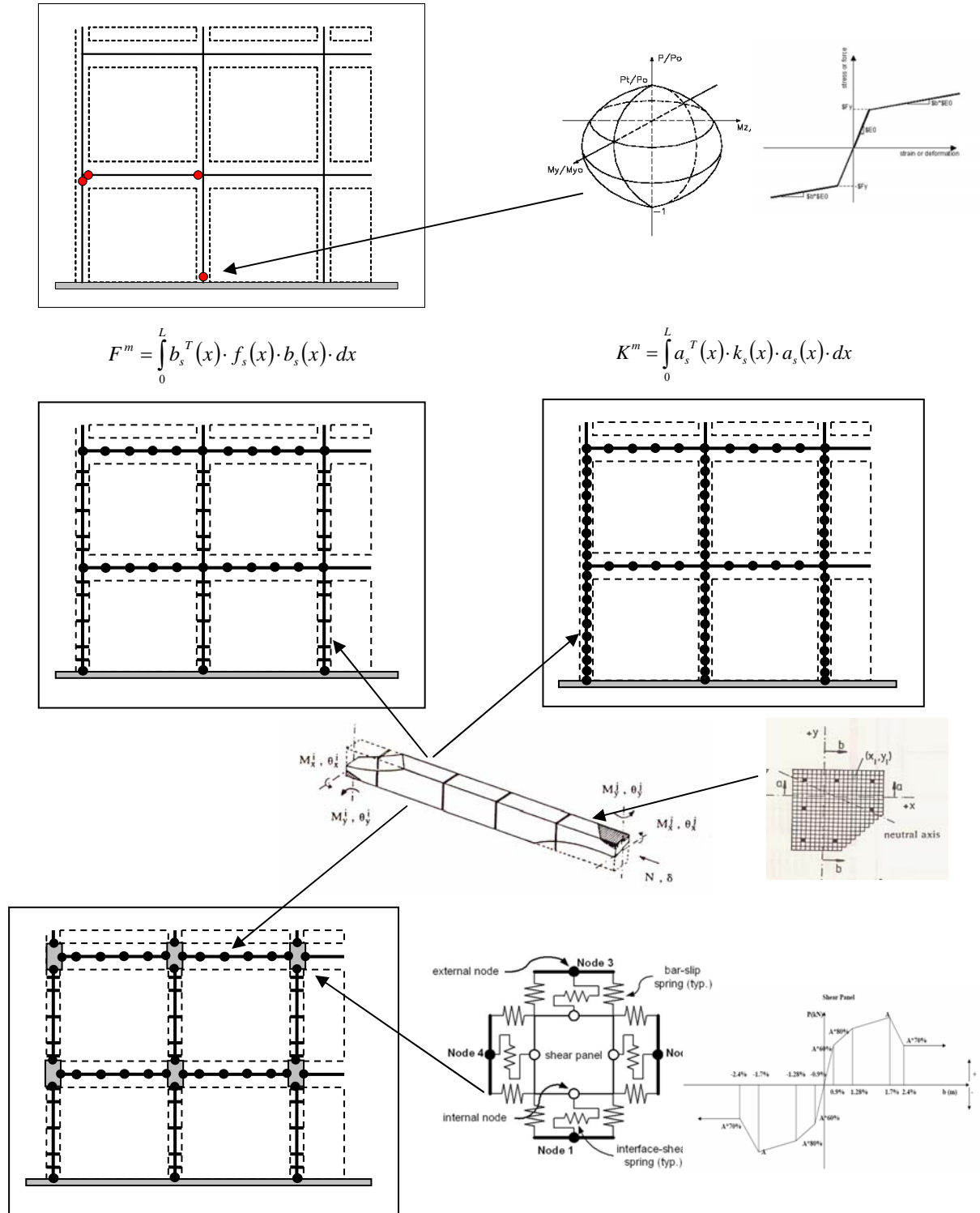


Figure 2: Schematic representations of the model formulations of the example building.

The distributed damage FE models denoted Disp, Force, Constant_hinge and Disp_Large_Deformation monitor damage (concrete cracking, spalling and crushing or reinforcement yielding) internally at control sections along their length [13,14]; following their respective element conventions, Disp and Force sections are located at the ends and at the Gauss-Lobato integration locations [14] – five sections for columns and three for beams being used, due to the higher element refinement in the beams. Disp_Large_Deformation elements use three internal sections positioned at the Gauss integration location (not at the ends), requiring therefore a higher element discretization per member: four elements per column are used (program default) and the same beam discretization as for Disp and Force. Finally, Constant_hinge elements adopt uniform properties over the user defined plastic hinge length, while the remaining portion of the element remains elastic. In all cases, steel bars are individually defined while core and cover concrete are modelled separately [11]. Sections are discretized between sixty (Disp, Force) to two hundred fibers (program default, Disp_Large_Displacement).

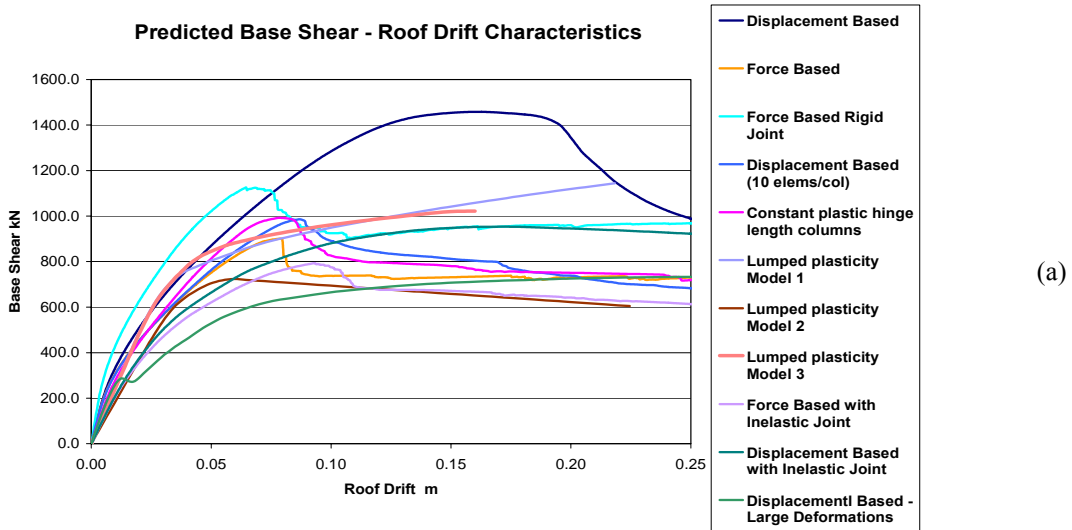
2.4 Joint FE modeling conventions

In addition to the above modeling techniques for the main structural elements, the structural joints of the different FE structural models were also represented explicitly in the various models following several alternative common engineering assumptions:

- i) All inframing members are assumed to join at the center (jt_model), excluding any explicit joint modeling;
- ii) All inframing members join at infinitely stiff and infinitely strong joints, through elastic offsets with dimensions equal to half the inframing member width (or depth); artificially rigid elastic elements in series with the beams and columns are used in this case (Opensees) or FE modeling capabilities (Drain 2DX);
- iii) Finally, flexible finite resistance joints are used (Opensees) with shear and flexural inelastic characteristics (Inl_jt model), capable of describing additional fixed end rotations due to interior bar slip within the body of the joint [15]. Shear deformations within the joint follow a trilinear hardening – bilinear softening load-deformation relation, at 60%, 80% and 100% of the maximum shear resistance, corresponding to a maximum shear stress of eight times the design shear stress (Fig. 2). The initial elastic shear stiffness is estimated with a Poisson ratio of 0.20 and joint cracking occurs at 0.9% strain. Steel reinforcement tensile bond-slip characteristics are modeled by assigning to the reinforcement springs a pinching material model with asymmetric properties in tension and compression: for tension, the anchored bar pullout behavior is evaluated following a uniform bond stress over the anchorage length, following [16]. To establish the spring stiffness in compression, 10% of the effective concrete compression area for the beams, or half the column width for the columns is added to the reinforcement stiffness, in order to represent the actual contact compression area in flexure for these two types of RC members.

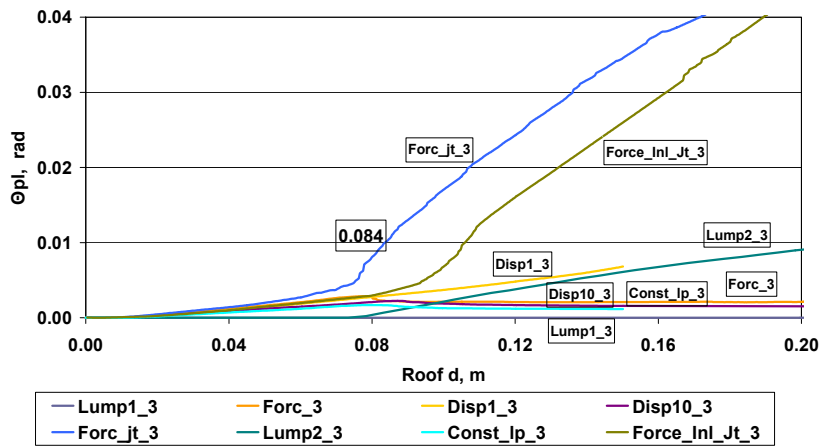
3 INELASTIC ANALYSIS PREDICTIONS

All the different FE models were analyzed using inelastic SPO analysis, under an imposed triangular profile of forces of increasing amplitude, or roof increasing lateral displacement control (or a mixture of these two methods, for the case of Lump_x). Depending on the analysis software, the inelastic solution iterative scheme is the tangent Newton-Raphson iteration with a specified convergence tolerance of 10^{-4} or an event – to event strategy, with automatic stiffness re-formulation at each step. Typically, the structure develops – by way of non conforming design – a soft story mechanism, whereby inelastic deformations are concentrated



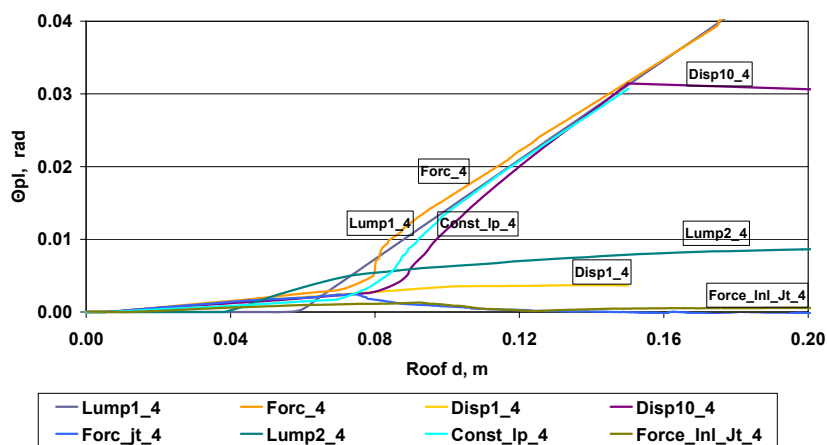
(a)

Plastic rotation demands with roof drift, 3rd Floor



(b)

Plastic rotation demands with roof drift, 4th Floor



(c)

Figure 3: Comparison of performance predictions under SPO Analyses of the different FE models: (a) Capacity curves, (b)-(c) Plastic rotational demands with imposed roof drift at the base of the exterior columns, third and fourth floor.

at the columns rather than the beams, primarily at the upper third and fourth floor. In Fig. 3(a), the resulting base shear versus roof drift capacity diagrams are plotted for all cases considered. In order to clearly demonstrate the collapse pattern depicted by each model, the variation of imposed (or derived) global roof drift with local plastic rotations (denoted θ_{pl}) at the base of the outermost perimeter columns, at the third and fourth floors on the tension side of the building, are compared in Fig. 3(b) and 3(c). The variation of local plastic rotation in these storey columns is in most cases the dominating inelastic demand among all the RC members of the frame; for PBD redesign purposes, the maximum inelastic rotation limit of 0.01 rad for non conforming elements is noted, following PBD evaluation per ATC-40 [1]. Due to the overturning effect of the lateral load and the small tributary slab areas, the columns under investigation suffer a gradual monotonic reduction in axial load with increasing lateral sway.

In Fig. 3(a), the variation of the predicted base shear – roof drift characteristics between the different FE formulations is examined. For the Lump_1,2 models the gross section moment of inertia is used for the columns and one half of the gross stiffness is used for the beams; all the spread damage models account for initial section cracking, through the concrete fiber constitutive characteristics, having similar constitutive behavior. Generally, all capacity curves exhibit some initial stiffness (and period) variability, with the Disp_Large_Deformation model being the softest (beams and columns in frame at the joint center in this case), with a pronounced cracking stiffness transition around 280 kN. No model exhibits a pronounced stiffness transition at onset of element yield, occurring at the lower floor beams in. Model Force with beam-column joints assumed to be non-deformable (Force_jt) exhibits the highest initial stiffness. This model also exhibits a higher peak lateral resistance, compared to Force, which is primarily attributed to a modification of the failure mechanism compared to its flexible counterpart, as subsequently described (see also Fig. 3(b)).

The peak base shear strength of the different models are reached at around 8 cm roof drift, yet they differ significantly between each other: The Force, Lump and Constant_Hinge models exhibit similar SPO characteristics, with a direct influence of the critical columns' post ultimate softening behavior to the overall global response (Fig. 3(a)). Unlike the majority of analyses, Disp_1 model exhibits similar initial response but a peak base shear resistance which is 50% higher than model Force, as well as considerably higher deformability than the latter. Disp_1 reaches ultimate strength at 16cm drift, exhibiting a monotonically increasing SPO profile up to 19cm where softening occurs, a fact that will affect its target point magnitude during PBD evaluation. With the exception of Disp1 and Disp1_Inelastic_Joint, all spread damage models eventually converge to similar post-ultimate resistance levels, between 600 and 700 kN. The Lump_1,2 and Force_Inelastic_Joint models exhibit the highest sensitivity to second order effects at this point (particularly softer model Lump_2).

The difference in local plastic rotation estimation as well as the roof deformation whereby the maximum inelastic rotational limit of 0.01 rad is exceeded for the different models, is examined by considering the θ_{pl} demands versus imposed roof drift at the base sections of the tension side perimeter columns at the third and fourth story, in Fig. 3(b) and 3(c). Different models exhibit different apparent collapse mechanisms: the Force, Lump_1 and Constant_Hinge models depict a soft story mechanism at the fourth floor, while model Disp_1 exhibits a uniform rotational demand distribution among the two floors, well below the maximum allowable limit up to 25cm drift imposed. Notably, the use of finite stiffness joint properties (models Force_jt and Force_Inelastic_Joint), results in a completely different collapse pattern, whereby third floor columns exhibit the highest θ_{pl} in this case. For Lump_1 and Lump_2, it is also observed that a change in the post yield hardening stiffness of the members, without affecting their flexural capacities, results in a modification of the collapse mechanism, with a more pronounced soft storey forming at the fourth floor (Lump_1) unlike Lump_2.

As far as the $Disp_x$ formulation is concerned, it is only after the discretization of the columns ($Disp_1$) is increased to ten elements per column ($Disp_{10}$), that the SPO curves of the Force and $Disp_{10}$ models converge. As depicted in Fig. 4(a) and 4(b), increasing the FE refinement of the elements where inelastic action concentrates, has a considerable influence on

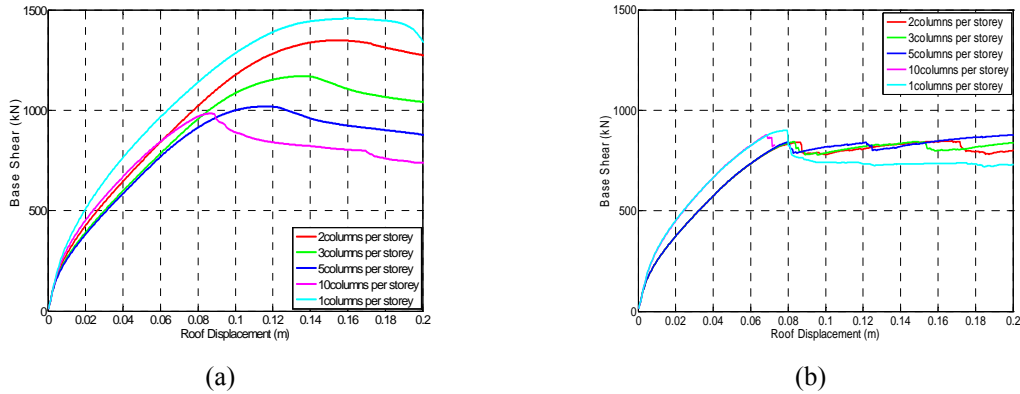


Figure 4: Comparison of performance predictions using different FE models. Column FE refinement sensitivity for (a) $Disp_x$ and (b) Force FE model formulations.

the capacity curve for the $Disp_x$ formulation unlike the Force model, for which using more than one element per column has no accuracy gain either global or local. Still, the fourth story column θ_{pl} of $Disp_{10}$ is underestimated by 35%: while models Lump2, Force and Constant_hinge predict a violation of the limiting value of 0.01 rad at 8.3 cm drift, the $Disp_{10}$ model reaches this value at 9.8 cm, with the former having reached a θ_{pl} of 0.015 rad by then.

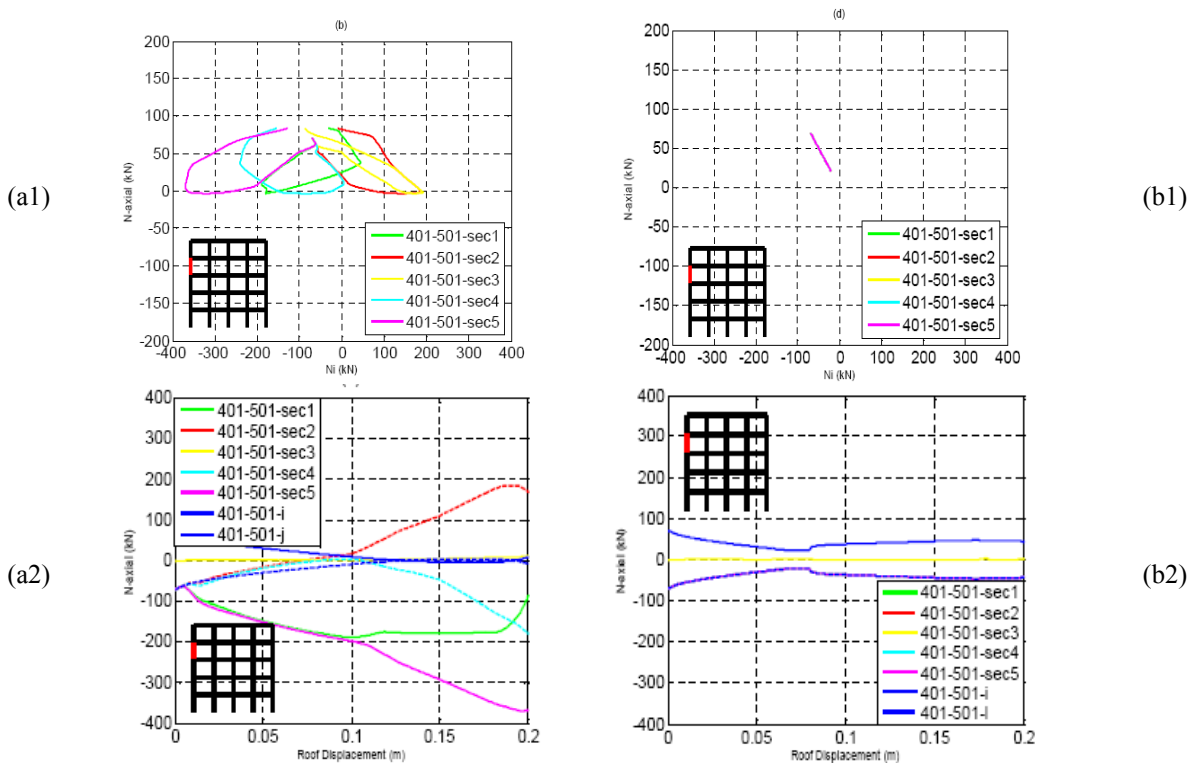


Figure 5: Variation of : 1) element axial loads and internal section action histories and 2) axial load with imposed roof deformation, fourth story exterior frame column; (a) $Disp_1$ model and (b) Force models.

The apparent high stiffness and strength of the Disp_1 as compared to the Force model, as previously discussed in [17], is demonstrated by considering the internal equilibrium state of the five monitored sections at the Gauss-Lobato points of the typical fourth floor perimeter column at the tension side of the building, whose end rotations are depicted in Fig. 3(c): as shown in Fig.5, while for the Force model axial loads remain constant over all five sections throughout the analysis, close to the end forces (Fig. 5(b2)), the axial loads of the Disp_1 sections diverge considerably from the end nodal values, reaching force levels as high as 400 kN compression, near the drift at peak resistance of the structure. Similarly, the moment – axial load traces of the internal sections in Fig. 5(a1) – 5(b1), demonstrate the apparent over-strength of the Disp_1 model’s critical regions – following heavy axial stressing – that result in a weighted increase in capacity of the element and potentially the entire building.

4 CONCLUSIONS

- Wide discrepancies may be expected in the inelastic FE response prediction by using: a) different FE models, such as lumped or spread plasticity, inelastic joints, use or not of in-fill elements; b) different modeling conventions, such as the use of stiff or rigid joints for the structural joints, c) use of large displacement formulations within the member FE model or d) discretization refinement of RC members (for displacement based models).
- SPO predictions of roof drift – local θ_{pl} dependencies exhibit a strong variability between different FE model formulations. Maximum θ_{pl} predictions at a global roof drift of 1% may vary by 100%. Refining the size of the displacement formulations to 10% the column length approximates better the global capacity curve, as obtained using flexibility element predictions, while enforcing better internal equilibrium. Predictions of θ_{pl} are still off by 35% however. Similarly, different soft storey type collapse patterns are predicted between different floors (third and fourth) of the five story structure.
- Overall, flexibility interpolation (force based) models exhibit higher demands and lower capacities compared to stiffness based elements, unless large displacement corrections are adopted internally in the latter and a large internal element discretization. Stiffness based elements exhibit large internal equilibrium errors in the monitored sections, a fact that will lead to improper target point estimation and numerical instability – depending on the degree of section softening. Force based models yield inelastic SPO predictions which are comparable to those obtained from lumped plasticity formulations. Previous analytical results, not reported herein, considering dynamic analysis predictions for these alternative models, revealed that this is not the case under dynamic excitation.
- The uncertainties introduced in the prediction of seismic performance strictly due to FE modeling only are significant, both under static or dynamic load analysis, even if common modeling assumptions and FE models widely adopted in practice are followed. For the same structural configuration, use of alternative FE modeling schemes and commonly adopted structural modeling techniques yielded different collapse patterns, collapse mechanism and global to local inelastic deformation relationships.
- Predicted collapse mechanisms and demanded plastic rotation magnitudes should therefore be interpreted with caution and engineering judgment rather than as hard performance indices for PBD acceptance of existing RC structures. For a practical application of PBD, the FE models for estimating acceptance or rejection of a structure should also become part of the PBD evaluation standardized procedures, when these adopt inelastic (re)analysis methods for structural evaluation.

REFERENCES

- [1] Applied Technology Council, Seismic Evaluation and Retrofit of Reinforced Concrete Buildings, Report ATC 40 / SSC 96-01, Palo Alto, California, 1996.
- [2] FEMA, NEHRP Guidelines for the Seismic Rehabilitation of Buildings, FEMA-273; and NEHRP Commentary on the Guidelines for the Seismic Rehabilitation of Buildings, FEMA-274, Federal Emergency Management Agency, Washington, D.C., 1997.
- [3] FEMA, Improvement of Nonlinear Static Seismic Analysis Procedures, FEMA-440, Federal Emergency Management Agency, Washington, D.C., 2005.
- [4] D. Vamvatsikos, C. A. Cornell, Incremental dynamic analysis, *Earthquake Engineering and Structural Dynamics*, **31**, 3, 491–514, 2002.
- [5] RD59 (1959), Earthquake Design Regulation of Building Works, Ministry of Public Works, Athens, Greece (in Greek).
- [6] C. Zeris, P. Giannitsas, K. Alexandropoulos, D. Vamvatsikos, Inelastic Modeling Sensitivity of the Predicted Seismic Performance of an Existing RC Building, Paper No: 980, *Proc. Thirteenth European Conference on Earthquake Engineering*, Geneva, 2006.
- [7] K. Repapis, C. Zeris, E. Vintzeleou, Evaluation of the Seismic Performance of Existing RC Buildings: II A Case Study for Irregular and Regular Buildings. *European Journal of Earthquake Engineering*, **10**, No 3, 429-452, 2006.
- [8] R. Allahabadi, G. Powell, DRAIN-2DX: User's Guide, Earthquake Engineering Research Center Report EERC 88-06, *University of California*, Berkeley, 1988.
- [9] F. McKenna, G. L. Fenves, B. Jeremic, M. H. Scott, Open system for earthquake engineering simulation (<http://opensees.berkeley.edu>), 2000.
- [10] S. Antoniou, R. Pinho, Seismostruct v.4.0.2, (<http://www.seismosoft.com>), 2006.
- [11] J. B. Mander, M. J. N. Priestley, R. Park, Theoretical stress-strain model for confined concrete, *Journal of the Structures Division, ASCE*, **114**, No 8, 1804–1826, 1988.
- [12] B.A. Izzuddin, Conceptual issues in geometrically nonlinear analysis of 3D framed structures, *Computer Methods in Applied Mechanics and Engineering*, **191**, 1029-1053, 2001.
- [13] A. Neuenhofer, F. C. Filippou, Evaluation of nonlinear frame finite-element models, *Journal of Structural Engineering, ASCE*, **123**, No 7, 958–966, 1997.
- [14] E. Spacone, F. C. Filippou, F. F. Taucer, Fibre beam-column element for nonlinear analysis of R/C frames. Part I: Formulation, *Earthquake Engineering and Structural Dynamics*, **25**, 711–725, 1996.
- [15] L. N. Lowes, N. M. Arash, A. Altoontash, A Beam-Column Joint Model for Simulating the Earthquake Response of Reinforced Concrete Frames, *Report 2003/10, PEER, University of California*, Berkeley, 2004.
- [16] S.-S. Lai, G. T. Will, S. Otani, Model for Inelastic Bi-axial Bending of Concrete Members, *Journal, Structural Engineering Division, ASCE*, **110**, 11, 2563-2584, 1984.
- [17] C. Zeris, S. Mahin, Analysis of Reinforced Concrete Beam-Columns Under Uniaxial Excitations, *Journal of the Structures Division, ASCE*, **114**, No 4, 1988.